Low-energy photodisintegration of the deuteron and Big-Bang nucleosynthesis

W. Tornow [a,b], N.G. Czakon [b], C.R. Howell [a,b], A. Hutcheson [a,b], J.H. Kelley [c,b],
V.N. Litvinenko [a,d], S.F. Mikhailov [a,d], I.V. Pinayev [a,d], G.J. Weisel [e], H. Witała [f]

[a] *Physics Department, Duke University, Durham, NC 27708, USA*
[b] *Triangle Universities Nuclear Laboratory, Durham, NC 27708, USA*
[c] *Physics Department, North Carolina State University, Raleigh, NC 27695, USA*
[d] *Duke University Free-Electron Laser Laboratory, Durham, NC 27708, USA*
[e] *Physics Department, Penn State Altoona, Altoona, PA 16601, USA*
[f] *Institute of Physics, Jagiellonian University, PL-30059 Cracow, Poland*

Abstract

The photon analyzing power for the photodisintegration of the deuteron was measured for seven gamma-ray energies between 2.39 and 4.05 MeV using the linearly polarized gamma-ray beam of the high-intensity gamma-ray source at the Duke Free-Electron Laser Laboratory. The data provide a stringent test of theoretical calculations for the inverse reaction, the neutron–proton radiative capture reaction at energies important for Big-Bang nucleosynthesis. Our data are in excellent agreement with potential model and effective field theory calculations. Therefore, the uncertainty in the baryon density $\Omega_B h^2$ obtained from Big-Bang Nucleosynthesis can be reduced at least by 20%.
© 2003 Published by Elsevier B.V. Open access under CC BY license.

Big-Bang nucleosynthesis (BBN) is an observational cornerstone of the hot Big-Bang (BB) cosmology. According to [1] the neutron(n)–proton(p) capture reaction $p(n, \gamma)d$ with a deuteron (d) and a 2.225 MeV γ ray in the exit channel is of special interest, because the BB abundance of deuterium provides direct information on the baryon density in the early universe at times between about 0.01 and 200 seconds

after the BB. Knowing accurately the n–p capture cross section in the energy range from 25 to 200 keV in the center-of-mass (c.m.) system and using the experimental value for the primeval deuterium number density $(D/H)_p$ [2,3], would allow for an accurate determination of the baryon density $\Omega_B h^2$ (h is the Hubble constant in units of 100 km s^{-1} Mpc^{-1}). From $\Omega_B h^2$ one can predict the abundances of the three light elements ^{3}He, ^{4}He, and ^{7}Li. According to [1], the 10% uncertainty in the deuterium-inferred baryon density $\Omega_B h^2 = 0.019 \pm 0.002$ comes in almost equal parts from the (D/H) measurements and theoretical uncer-

E-mail address: tornow@tunl.duke.edu (W. Tornow).

tainties in predicting the deuterium abundance. For the latter, the knowledge of the n–p capture cross section is of crucial importance. Unfortunately, there is a near-complete lack of data at energies relevant to BBN. Aside from thermal energies, data exist only at n–p c.m. energies of 275 keV and above. As a consequence, the ENDF-B/VI [4] evaluation has been used [1] in the BBN energy range. This evaluation is normalized to the high-precision thermal n–p capture cross-section measurements. The 5% uncertainty that is assigned in this approach contributes a significant fraction to the uncertainty in the baryon density and consequently in the abundances of the light elements produced in BBN.

Very recently, with the precision results from WMAP (Wilkinson Microwave Anisotropy Probe) for the Cosmic Microwave Background (CMB) and its anisotropies an independent and even more accurate result became available: $\Omega_B h^2 = 0.0224 \pm 0.0009$ [5,6]. The comparison of the baryon density predictions from BBN and the CMB is a fundamental test of BB cosmology [7]. Any deviation points to either unknown systematics or the need for new physics. Therefore, it is of crucial importance to reduce the uncertainty in $\Omega_B h^2$ obtained from BBN. As stated above, 50% of the uncertainty is due to the uncertainty in the n–p capture cross section in the energy range of interest.

Recently, effective field theory approaches [8,9] have provided accurate results for the time-reversed reaction γ–$d \rightarrow n$–p from threshold (2.225 MeV) to about 10 MeV incident γ-ray energy. The work described in this Letter was motivated by these new theoretical results and also earlier nucleon–nucleon potential model based calculations [10] in the γ-ray energy range important to BBN ($E_\gamma = 2.25$–2.43 MeV). Aside from the γ–d cross section, and the n–p capture cross section inferred via "detailed balance", these calculations predict results for other observables as well which are related to the cross section, but are in principle experimentally easier to measure with high accuracy than the n–p capture cross section itself. The aim of this work is to provide an alternative method of determining the accuracy of theoretical models in predicting the n–p capture cross section in the energy range of interest for BBN. Potentially, this could lead to a considerably smaller uncertainty in $\Omega_B h^2$ obtained from BBN.

We measured the analyzing power $\Sigma(90°)$ for the $^2\text{H}(\vec{\gamma}, np)$ reaction with linearly polarized γ-rays at $\theta = 90°$ (lab) for seven energies between $E_\gamma = 2.39$ and 4.05 MeV. This energy range corresponds to n–p c.m. energies of 165 keV to 1.83 MeV, i.e., the present experiment includes for the first time data in the upper energy range of interest to BBN. The analyzing power $\Sigma(\theta)$ is defined as

$$\Sigma(\theta) = \frac{\sigma(\theta, \phi = 0°) - \sigma(\theta, \phi = 90°)}{\sigma(\theta, \phi = 0°) + \sigma(\theta, \phi = 90°)} \frac{1}{f}$$
$$= \frac{b \sin^2 \theta}{a + b \sin^2 \theta} \frac{1}{f},$$

where the differential cross section $\sigma(\theta, \phi)$ is given by

$$\sigma(\theta, \phi) \sim a + b \sin^2 \theta \, [1 + \cos 2\phi].$$

Here, θ is the polar angle, ϕ is the azimuthal angle, and f is the degree of linear polarization of the incident γ-ray beam. The quasi-monoenergetic and linearly polarized γ-ray beam was produced by Compton backscattering of relativistic electrons from 670 nm free-electron laser (FEL) photons at the High-Intensity Gamma-ray Source (HIGS) located at the Duke University Free-Electron Laser Laboratory. The electron energy in the electron storage ring was varied between $E_e = 300$ and 375 MeV to generate γ-ray beams of energy between 2.39 and 4.05 MeV. At a distance of 75 m from the electron–FEL–photon collision point the collimated γ-ray beam of 2.6 cm diameter struck a 4 cm diameter and 6 cm long deuterated liquid scintillator (C_6D_{12}, Nuclear Enterprises NE232) contained in a thin-walled glass container and viewed by a photomultiplier tube (PMT). The axis of the scintillator-PMT arrangement coincided with the axis of the incident γ-ray beam. The average γ-ray flux at the location of this deuterated scintillator target (DST) was $5 \times 10^5 \, \gamma/s$. The γ-ray beam was monitored with a 140% HPGe detector positioned downstream of the experimental setup. Aside from low-energy γ-ray sources the "natural" γ-ray lines at $E_\gamma = 1461$ keV (^{40}K) and $E_\gamma = 2614.5$ keV (^{208}Tl) served as convenient online calibration sources throughout the course of the experiment. The energy spread $\Delta E / E$ of the γ-ray beam varied between 2.3% FWHM at $E_\gamma = 2.39$ MeV to 2.9% FWHM at $E_\gamma = 4.05$ MeV.

The experimental setup is shown schematically in Fig. 1. Neutrons from the deuteron breakup reaction
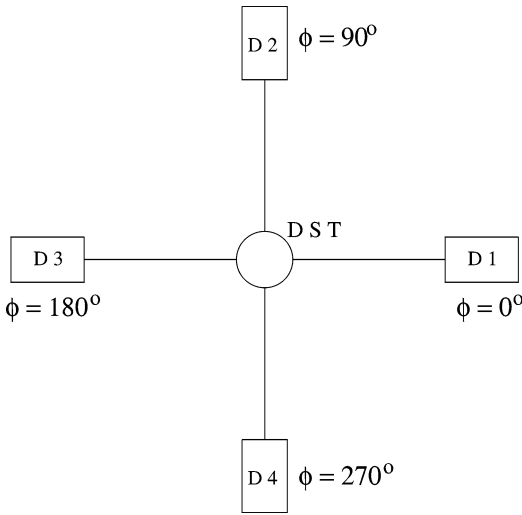
Fig. 1. Schematic of experimental setup. The γ-ray beam is perpendicular into the page and the γ-ray polarization is nominal in the $\phi = 0$ plane.
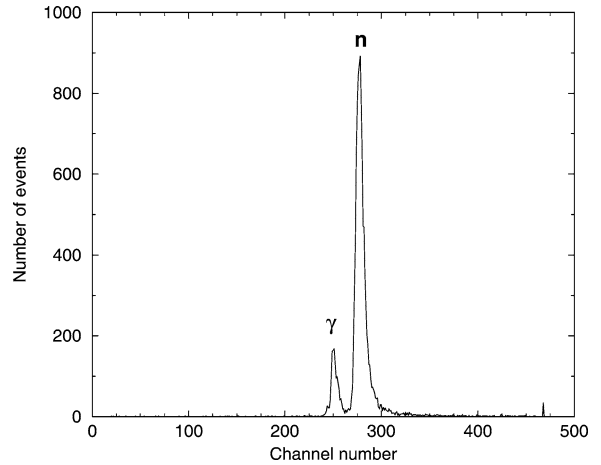

Fig. 2. Neutron time-of-flight spectrum between the deuterated scintillator and a neutron detector for the reaction $\gamma - d \rightarrow n - p$ at $E_\gamma = 4.05$ MeV. Time increases from left to right. The dominant peak is due to the neutrons of interest. The small peak is due to γ rays leaking through the PSD cut. This leakage is smaller than 0.1%.
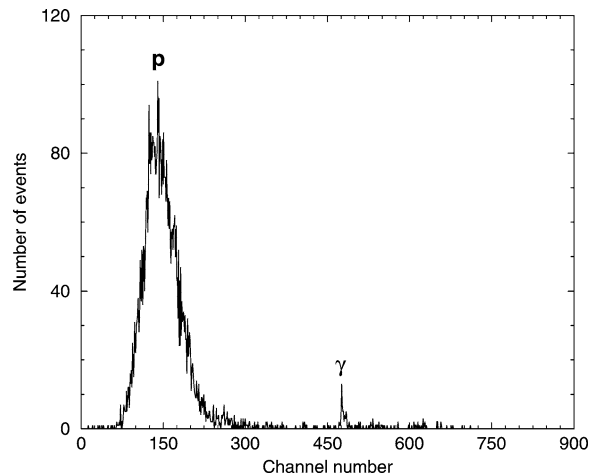

Fig. 3. Proton recoil energy spectrum in the deuterated scintillator (DST) at $E_\gamma = 4.05$ MeV. The small peak near channel 450 is due to electrons generated via Compton scattering to the neutron detector.

were detected by four Bicron 501A liquid scintillator detectors, $2''$ in diameter and $2''$ in length, viewed by a PMT. We used four detectors rather than two to increase the efficiency of our experimental setup. Two neutron detectors were mounted at $\theta_{\text{lab}} = 90°$ in the plane of the γ-ray polarization (nominally the horizontal plane) on opposite sides of the incident γ-ray beam ($\phi = 0°$ and $180°$). The other two detectors were mounted at $\theta_{\text{lab}} = 90°$ in the perpendicular plane ($\phi = 90°$ and $270°$). The center-to-center distance between the DST and the neutron detectors was 17 cm. The protons from the deuteron breakup in the DST gave the start signal for a neutron time-of-flight measurement between the DST and the neutron detectors. Neutron–gamma pulse-shape discrimination (PSD) techniques were applied to distinguish the events of interest from the overwhelming background produced in the neutron detectors by Compton scattering from the DST. Two-dimensional spectra of pulse height in the DST versus neutron time-of-flight were created for the four neutron detectors used in the present experiment. Time-of-flight and proton recoil energy spectra are shown in Figs. 2 and 3 for an incident gamma-ray energy of 4.05 MeV. Our experimental techniques cannot be extended to much lower γ-ray energies than already achieved in the present experiment. At $E_\gamma = 2.39$ MeV both the proton and neutron

energies were only 90 keV compared to the more comfortable value of about 900 keV at $E_\gamma = 4.05$ MeV. Liquid scintillator detectors are not commonly employed to detect neutrons and protons at energies of less than 500 keV. However, other types of detectors lack the fast timing characteristics and efficiencies that are crucial for obtaining $\gamma - d$ data in the energy range between $E_\gamma = 2.4$ and 3 MeV.

In order to cancel instrumental asymmetries in our experimental setup, we either rotated the neutron detectors which were mounted on a ring centered and positioned perpendicular to the γ-ray beam axis through 90° (counter clockwise), or we interchanged the detectors, i.e., the detectors in the horizontal plane were moved to the vertical plane and vice versa. Within statistical uncertainties either procedure gave consistent results for the asymmetry ϵ, which was calculated from the formula $\epsilon = (\alpha - 1)/(\alpha + 1)$. For the rotation procedure we defined α as

$$\alpha_{1\text{--}2} = \left[\left(N_1^{\mathrm{HR}} N_2^{\mathrm{HL}}\right) / \left(N_2^{\mathrm{VU}} N_1^{\mathrm{VU}}\right)\right]^{1/2}$$

for detector pair 1–2, and as

$$\alpha_{3\text{--}4} = \left[\left(N_3^{\mathrm{HL}} N_4^{\mathrm{HR}}\right) / \left(N_4^{\mathrm{VD}} N_3^{\mathrm{VD}}\right)\right]^{1/2}$$

for detector pair 3–4. Similarly, for the interchange procedure we have

$$\alpha_{1\text{--}2} = \left[\left(N_1^{\mathrm{HR}} N_2^{\mathrm{HR}}\right) / \left(N_2^{\mathrm{VU}} N_1^{\mathrm{VU}}\right)\right]^{1/2}$$

for detector pair 1–2, and

$$\alpha_{3\text{--}4} = \left[\left(N_3^{\mathrm{HL}} N_4^{\mathrm{HL}}\right) / \left(N_4^{\mathrm{VD}} N_3^{\mathrm{VD}}\right)\right]^{1/2}$$

for detector pair 3–4. Here, $N_i^{\mathrm{HR}}(N_i^{\mathrm{HL}})$ refer to the neutron yields detected with detector i positioned in the horizontal plane to the right (left) side of the incident γ-ray beam, and $N_i^{\mathrm{VU}}(N_i^{\mathrm{VD}})$ refer to the neutron yields detected with detector i positioned in the vertical plane in the up (down) position.

Based on the geometry of the undulator magnets used to produce the FEL photons, the photon polarization should be linear and of magnitude 1.0. Furthermore, the polarization plane should coincide with the horizontal plane in the laboratory. Using the polarization dependent formulas for inverse Compton scattering this should result in a linear γ-ray polarization in the horizontal plane of $f = 1.0$ in the photon and electron energy range of interest for the present experiment. However, the optical cavity mirrors used to produce the FEL photons of 670 nm were optically active, causing a rotation of the polarization plane of the FEL photons and consequently of the resulting γ-ray beam. The outcoupled FEL light was used to verify the linear polarization of 1.0 and to determine the tilt angle of the polarization plane. However, there is no guarantee that the tilt angle of the polarization plane of the outcoupled light (i.e., the transmitted light through the mirror opposite to the γ-ray beam direction) is in perfect

agreement with the tilt angle of the FEL photon polarization inside of the optical cavity where the electron–photon collision takes place. Therefore, the tilt angle of the γ-ray polarization plane relative to the nominal horizontal plane was determined from the measured asymmetry ϵ of the Compton scattered γ rays by setting the PSD gate on the γ rays in the neutron detectors and by selecting the appropriate pulse height gate (due to γ-ray scattering from electrons through 90°) in the DST. This asymmetry ϵ was determined simultaneously with the one for the breakup neutrons from the γ–d reaction. In order to extract the tilt angle from the measured γ-ray asymmetry data, the effective analyzing power of our apparatus for Compton scattering from electrons was calculated via Monte-Carlo simulation using the Klein–Nishina formula. The polarization in multiple Compton scattering was treated exactly. The average tilt angle of the γ-ray polarization plane was found to be $(13.7 \pm 0.2)°$ in upward direction relative to the horizontal laboratory plane. This value is about 2° larger than the polarization tilt angle of the outcoupled FEL photons.

The neutron asymmetry data from the γ–$d \rightarrow n$–p reaction were corrected for finite geometry and multiple-scattering effects via extensive Monte-Carlo simulations of the experimental setup, using the tilt angle of the γ-ray polarization determined above and the γ–d cross section and analyzing power calculations of Arenhövel [10] which are based on the Bonn nucleon–nucleon potential model [11]. The use of an active deuterium target makes our data practically insensitive to multiple γ-ray scattering (i.e., Compton scattering off electrons) in the DTS before the γ–$d \rightarrow n$–p reaction of interest is taking place. The light output produced by the recoil electrons generated in the Compton scattering process is considerably larger than the light output produced by the protons from the γ–$d \rightarrow n$–p reaction. Therefore, multiple γ-ray scattering can be eliminated efficiently by setting a tight gate on the proton pulse height of interest. In contrast, multiple scattering of the neutrons from the γ–d reaction in the DST has to be taken seriously. Especially at the lowest γ-ray energies employed in the present experiment, our constraint on the proton pulse height in the DST and our cut on the neutron time-of-flight did not eliminate multiple scattering events completely due to limitations of the detectors' energy and time resolutions.

The data for the excitation function of the analyzing power $\Sigma(90°\ \text{lab})$ are shown in Fig. 4 and listed in Table 1. The error bars include statistical and systematic uncertainties added in quadrature. At the higher energies the analyzing power is close to 1, i.e., the neutrons are emitted almost completely in the plane of the γ-ray polarization (electric dipole radiation E1). At energies below $E_\gamma = 3$ MeV, $\Sigma(90°)$ decreases rapidly, i.e., the probability for neutrons to be emitted in the vertical plane (magnetic dipole radiation M1) increases with decreasing γ-ray energy. The curve shown in Fig. 4 is the prediction of Arenhövel [10] using the coordinate-space version of the Bonn nucleon–nucleon potential model [11]. The calculation includes meson-exchange, isobar, and relativistic effects. Clearly, the model calculation is in very good agreement with the experimental data. Table 1 shows that the effective field theory approach of Chen and Savage [8] gives basically the same results as the potential model calculation of Arenhövel.
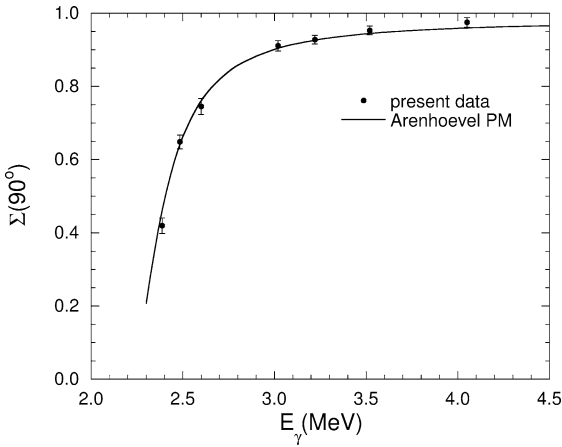
As shown in detail by Schreiber et al. [12] the γ–d analyzing power data $\Sigma(\theta)$ at low energies can be used to determine the relative M1 and E1 strengths of the γ–d cross section. Based on the present $\Sigma(90°\ \text{lab})$ data, Table 2 gives the calculated M1 contribution to the γ–d cross section in comparison to the effective-field theory calculations of Chen and Savage, Rupak [9], and the nucleon–nucleon potential-model calculation of Arenhövel. In the energy range most important for BBN our results are in excellent agreement with the theoretical predictions, especially with the calculations of Arenhövel. Fig. 5 shows the calculated total γ–d cross section of Chen and Savage as well as the associated M1 and E1 contributions in comparison to the M1 contribution determined in the present work (dots) and in the earlier work of Schreiber et al. at $E_\gamma = 3.58$ MeV (triangle).

In summary, the first experimental test of theoretical models used to calculate the n–p capture cross section in the energy range of importance to BBN reveals almost perfect agreement with experimental in-

Fig. 4. Excitation function of the photon analyzing power Σ for the reaction γ–$d \rightarrow n$–p at $\theta_{\text{lab}} = 90°$ in comparison to the theoretical prediction of Arenhövel.

Table 2

M1 (s-wave) contribution S to the total γ–d cross section obtained from the present $\Sigma(\theta)$ data in comparison to the predictions of Arenhövel, Chen and Savage, and Rupak

E_γ	S			
(MeV)	This experiment	Arenhövel	Chen & Savage	Rupak
2.39	0.675 ± 0.019	0.662	0.622	0.627
2.48	0.448 ± 0.020	0.468	0.459	0.458
2.60	0.339 ± 0.026	0.328	0.320	0.317
3.02	0.128 ± 0.019	0.141	0.139	0.135
3.22	0.104 ± 0.017	0.108	0.109	0.104
3.52	0.069 ± 0.017	0.080	0.083	0.079
4.05	0.037 ± 0.019	0.057	0.061	0.056

Table 1

Measured photon analyzing power Σ at $\theta_{\text{lab}} = 90°$ in comparison to theoretical predictions

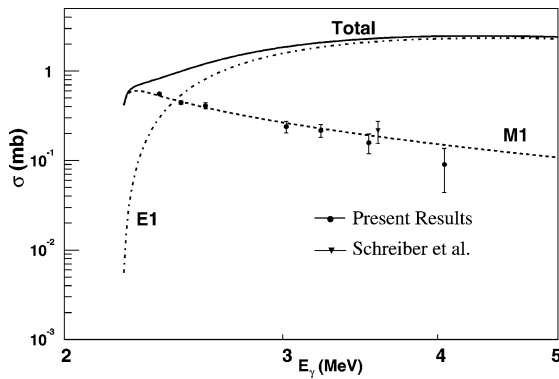| E_γ (MeV)	$\theta_{\text{c.m.}}$ (deg)	$E_{\text{c.m.}}^{n-p}$ (keV)	Σ	$\Sigma_{\text{Arenhövel}}$	$\Sigma_{\text{Chen \& Savage}}$
2.39	95.6	165	0.419 ± 0.021	0.461	0.464
2.48	94.6	255	0.649 ± 0.019	0.624	0.631
2.60	94.0	375	0.745 ± 0.022	0.760	0.757
3.02	93.2	795	0.911 ± 0.014	0.902	0.901
3.22	93.0	995	0.928 ± 0.012	0.925	0.923
3.52	92.9	1295	0.953 ± 0.012	0.944	0.942
4.05	92.8	1825	0.975 ± 0.013	0.959	0.958

Fig. 5. Data for the M1 contribution to the γ–d total cross section in comparison to the theoretical prediction of Chen and Savage (dashed curve). The dashed-dotted curve represents the E1 contribution and the solid curve in the total γ–d cross section from Chen and Savage. Note the logarithmic scales for both σ and E_γ.

formation derived from analyzing power data for the reverse reaction γ–$d \rightarrow n$–p. This observation lends substantial credibility to the theoretical models also in the presently not tested γ-ray energy range from 2.25 to 2.38 MeV, i.e., for n–p c.m. energies between 25 and 155 keV. Work is planned to reduce the uncertainty of the described measurements from its present 3% uncertainty at 2.39 MeV in determining the dominant M1 contribution to the γ–d cross section to 1.5% and to extend the measurements to n–p c.m. energies as low as 25 keV.

We conclude that the $\pm 5\%$ uncertainty used in [1] is a very conservative estimate for the uncertainty of modern theoretical approaches available for calculating the n–p capture cross section in the energy range relevant to BBN. The uncertainty quoted in Ref. [1] can be reduced by at least 20%. The planned improvements of our measurements are expected to provide an even more accurate test of the calculated n–p capture cross section. Therefore, this cross section will play

a small role in the overall uncertainty of the baryon density in the early universe as determined in Ref. [1]. The BBN approach compares favorably with the very recent CMB based method of determining $\Omega_B h^2$ from the WMAP data [5,6].

Acknowledgements

References

[1] S. Burles, K. Nollett, J. Truran, S. Turner, Phys. Rev. Lett. 82 (1999) 4177.
[2] S. Burles, D. Tytler, Astrophys. J. 499 (1998) 699.
[3] S. Burles, D. Tytler, Astrophys. J. 507 (1998) 732.
[4] G. Hale, D. Dodder, E. Siciliano, W. Wilson, Los Alamos National Laboratory, ENDF/B-VI evaluation, Mat. No. 125, Rev. 2 (1997); ENDF data base at the NNDC Online Data Service.
[5] C. Bennett, et al., Astrophys. J., in press.
[6] D. Spergel, et al., Astrophys. J., in press.
[7] R. Cybert, B. Fields, K. Olive, astro-ph/0302431.
[8] J. Chen, M. Savage, Phys. Rev. C 60 (1999) 065205.
[9] G. Rupak, Nucl. Phys. A 678 (2000) 405.
[10] H. Arenhövel, M. Sanzone, Few-Body Systems Suppl. 3 (1991);
     H. Arenhövel, private communication.
[11] R. Machleidt, K. Holinde, C. Elster, Phys. Rep. 149 (1987) 1.
[12] E. Schreiber, et al., Phys. Rev. C 61 (2000) 061604.